



Research on the layout optimization and utilization of floor gas extraction roadway: a case study in Shoushan No.1 Coal Mine, China

Xiong Ding^{1,2} · Cheng Zhai^{1,2} · Jizhao Xu^{1,2} · Xu Yu^{1,2} · Yong Sun^{1,2} · Yuzhou Cong^{1,2} · Yangfeng Zheng^{1,2} · Wei Tang^{1,2}

Received: 18 January 2022 / Accepted: 10 June 2022 / Published online: 21 June 2022
© Saudi Society for Geosciences 2022

Abstract

Gas extraction with the crossing boreholes of the floor rock roadway is an important method to prevent accidents of coal and gas outbursts. The spatial layout of the floor gas extraction roadway has a specific impact on the pressure release and gas extraction efficiency of the target coal seam. Conventional layout designs of the floor gas extraction roadway did not organically combine with the coal seam mining and gas extraction design. This paper took Shoushan No.1 Mine in Pingdingshan as the research object to study the optimization and utilization of spatial layer layout of floor gas extraction roadway. The authors constructed numerical models to analyze the influence of the floor gas extraction roadway on the upper coal roadway during the study, took into account the synergistic effect of anti-outburst and mining, and combined the characteristics of the coal floor rock lithology and gas extraction. The results show that with the decrease in the horizontal and vertical distance between the floor gas extraction roadway and the upper pre-set coal roadway, the pressure relief effect of the pre-set coal roadway is evident. Meanwhile, the elastic strain energy accumulated in the unit volume of coal becomes small under the influence of the excavation of the lower floor gas extraction roadway. When arranged directly below the coal roadway, the floor gas extraction roadway is less affected by coal seam mining. Through comprehensive analysis of the numerical simulation results, the lithology of the coal seam floor, the demand for gas extraction, and the economic benefits of Shoushan No.1 Mine, the floor gas extraction roadway of the mechanical transport roadway was determined to arrange in the marl within the horizontal distance of 6 m and vertical distance of 8~12 m from the mechanical transport roadway. Finally, a comprehensive evaluation system for the layer selection of the floor gas extraction roadway with four aspects of “anti-outburst, stability, lithology, and extraction” was formed, which will provide a reference for other similar coal mine projects.

Keywords Floor gas extraction roadway · Layer selection · Numerical simulation · Prevention of outburst

Introduction

With the increase of coal mining depth, the mechanism of coal and gas outbursts and the destruction mechanism of deep roadways tend to be complicated (Yang et al. 2017), and the difficulty of gas control is increasing. There are two main types of regional anti-outburst measures in coal mines,

including mining protective seams and pre-extraction of coal seam gas (Zhou et al. 2016). It is an effective gas extraction method for pre-drainage gas through crossing boreholes of the floor gas extraction roadway (FGER) (Li et al. 2020a; Lu et al. 2014), effectively reducing the gas concentration in the coal seam and preventing the coal and gas outburst. However, under the influence of high temperature, high ground stress, and mining disturbance, the excavation of the FGER will result in increased displacement of the surrounding rock, large deformation and rheology, severe damage to the support structure, and difficulties in repairing the FGER (Tsesarsky et al. 2013; Wang et al. 2000). These problems seriously restrict the safe and efficient production of coal mines, so it is urgently needed to study the layout and comprehensive utilization of the FGER.

In recent years, scholars have conducted much research on the layout of floor roadways and the principle of roadway

Responsible Editor: Zeynal Abiddin Erguler

✉ Cheng Zhai
greatzc@cumt.edu.cn

¹ Key Laboratory of Coal Methane and Fire Control, Ministry of Education, China University of Mining and Technology, Xuzhou 221116, Jiangsu, China

² School of Safety Engineering, China University of Mining and Technology, Xuzhou 221116, Jiangsu, China

instability. Guo et al. (2021) elaborated on the distribution characteristics of the plastic zone of surrounding rock when the floor drainage roadway is located at different positions under the working face through numerical simulation and determined the appropriate location of the floor drainage roadway. Jiang et al. (2016), Li (2020), and Li et al. (2020b) studied the interaction between floor roadway and upper coal roadway, coal pillar, and dynamic mining area. The main methods to analyze the instability principle of floor roadway include numerical simulation, theoretical calculation, physical model simulation, and in situ test. Mo et al. (2020) examined the buckling mechanism of the roadway floor through numerical simulation methods to study the interaction between strong and weak floor slabs. Małkowski (2015) developed a numerical simulation algorithm to analyze the influence of the elastoplastic model on the damage to the surrounding rock structure of the roadway. Wang et al. (2000) proposed the principle of controlling the stability of the floor roadway according to the nature of the floor roadway in the weak stratum. Mu et al. (2019) explored the dynamic rupture mechanism of the coal seam floor based on the cusp mutation model of elastic thin plate theory. Wang et al. (2021) and Li et al. (2018) analyzed the failure mechanism and deformation characteristics of surrounding rock in the floor rock roadway under coal seam mining. Some researchers analyzed the deformation and failure characteristics and damage depth of the coal seam floor based on sensing technology, three-dimensional resistivity method, and seismic wave CT, obtained the calculation formula of the maximum depth of the mining fracture zone of the floor (Zhou et al. 2019; Si et al. 2020). Jeon et al. (2004), Lee and Wulf (2008), and Jing et al. (2020) studied the damage mechanism of roadway excavation and related problems by small-scale physical model tests. Some scholars have also designed different support methods according to the actual conditions of the coal mine site to improve the support strength to ensure the stability of the deep roadway (Wu et al. 2020; Shen 2013; Xue et al. 2017).

The spatial layout of the floor rock roadway has an important influence on preventing coal and gas outbursts during the excavation of the upper coal roadway and the pressure relief of the target coal seam. China's coal mining experience shows that more than 70% of gas outbursts occur during roadway excavation (Yang et al. 2018). Existing research results indicate that high ground stress and high gas pressure play an irreplaceable role in the coal and gas outbursts (Karacan et al. 2011; Moore 2012; Black 2019; Ranjith et al. 2017). Pan et al. (2020) and Tu et al. (2019) analyzed the effect of tectonics on the spatial distribution of coal seams. They explored the intrinsic mechanism and influence mechanism of tectonics and coal and outbursts. Recently, numerical simulation methods are also frequently used to study the mechanism of coal and gas outbursts (Liu et al. 2018; Tang

et al. 2021; Yu et al. 2014; Yu et al. 2020). Yang et al. (2018) used Flac3D to simulate the stress distribution in front of the coal roadway driving work and proposed a “strong-weak” coupling circle-layers to reduce the outburst risk when the roadway crosses a gas coal seam. Zheng et al. (2022) proposed a strong-weak coupling structure to improve coal excavation stability and reduce energy accumulation through numerical simulation and field experiments. Some scholars have also explained gas outbursts from the perspective of energy principles. Wei et al. (2021), Zhao et al. (2019), Lu et al. (2019), and Lei et al. (2020) considered the outburst process as a sudden release of the accumulated elastic strain energy and gas internal energy in coal.

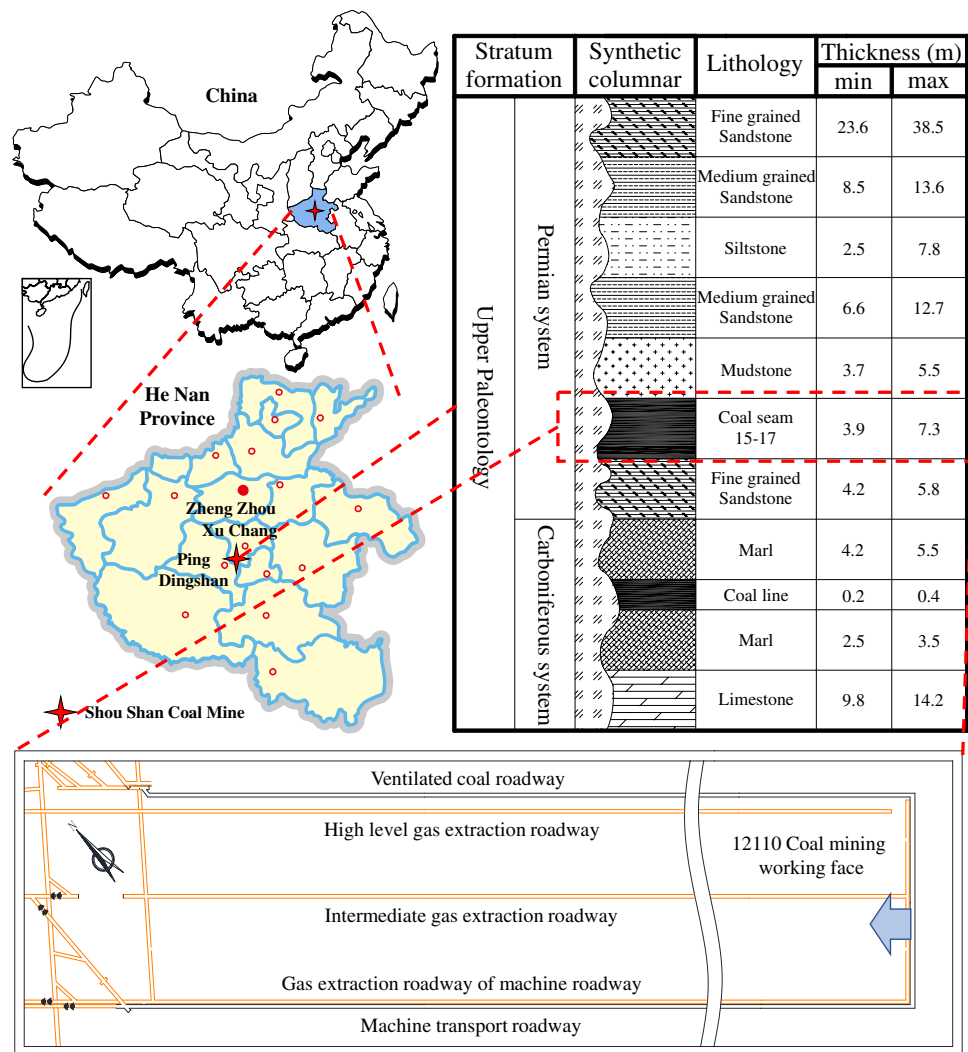
According to the above, although there are many achievements in the layout of roadways, few scholars combined the layer layout of the floor rock roadway with the spatial relationship between the upper coal roadway and the stability of the coal roadway and the floor rock roadway under the influence of mining. When studying the spatial layout of the floor roadway, the effect on the prevention of coal and gas outbursts in the upper coal roadway excavation and the pressure relief of the target coal seam is less involved. There is a lack of careful consideration in the layout and utilization of the FGER.

Choosing the suitable layer of FGER to ensure the safety of coal roadway excavation, stable roadway support, and extraction efficiency has become the critical, difficult point in managing methane disasters in high gas and low permeability coal seams. This paper took Shoushan No.1 Mine in Pingdingshan as the research object to study the optimization and utilization of spatial layer layout of floor gas extraction roadway. The authors constructed numerical models to analyze the influence of the floor gas extraction roadway on the upper coal roadway, took into account the synergistic effect of anti-outburst and mining, and combined the characteristics of the coal floor rock lithology and gas extraction. Finally, based on the numerical simulation and industrial experiments, a comprehensive evaluation system for selecting the FGER layer based on the four aspects of “anti-outburst, stability, lithology, and extraction” was formed, which will provide a reference for other similar coal mine projects.

Engineering background

Shushan No. 1 Coal Mine is a coal and gas outburst mine located in Henan Province, China. Figure 1 shows the mine location and the comprehensive column diagram of the coal and rock strata. The 15–17 coal seam is an outburst coal seam with a max original gas content of 11.2 m³/t and a max original gas pressure of 1.2 MPa. A total of 12,110 working face is the object of this study, with an average coal seam thickness of 5.6 m and a coal seam inclination angle of about

Fig. 1 Information of 12110 working face in Shoushan No. 1 Mine



5°. The construction method of “one working face and five roadways” was used for coal seam gas management, and the five roadways are one high-level gas extraction roadway, two FGERs, and two coal roadways.

The 15–17 coal seam belongs to a single outburst coal seam and does not have the mining conditions for a protective coal seam. It is proposed to carry out gas extraction by drilling crossing boreholes in the FGER to reduce the gas pressure and content. The FGER of mechanical transportation roadway can also reduce the risk of outburst at the working face of mechanical transportation roadway excavation.

From the lithology of the coal seam floor, the authors selected the suitable permissible range for the layout of the FGER of mechanical transportation roadway. Numerical simulations were conducted to analyze the influence of the FGER on the stability and anti-outburst effect of the upper coal roadway, the stability of the FGER under the influence of mining, and the practice of gas extraction. Based on the numerical simulation results and the gas extraction situation

at the site, the reasonable spatial layer layout of the FGER was determined.

Numerical simulation

There are two numerical simulations in this research conducted according to the actual geological conditions and mining situation of Shoushan No.1 Coal Mine. The first numerical simulation simulated the roadway excavation before coal seam mining. The second numerical simulation analyzed the damage to the coal seam floor affected by mining in the case with or without a FGER. The simulation software used is the FLAC3D6.0 software, which uses an explicit Lagrangian algorithm to simulate the plastic failure of coal and rock bodies at the yield limit during coal seam mining and roadway excavation in mining engineering. The computational model used is the Mohr-Coulomb model, which usually represents the shear damage of the soil-rock

body. The mechanical parameters of the rock formation used in the calculation are shown in Table 1. The model simulated the overlying rock layer of 900 m with a load of 23.5 MPa. The ground stress is mainly horizontal tectonic stress, with the maximum horizontal principal ground stress σ_H of about 40 MPa and the minimum horizontal principal ground stress σ_h of about 17 MPa.

Model analysis indicators

The authors used four model analysis indicators in numerical simulations to analyze the appropriate location of the FGER, including elastic strain energy, deformation coefficient, plastic zone distribution, and relative displacement.

Elastic strain energy

In coal mine gas prevention and control, the outburst of coal and gas that occurs during the tunneling of coal roadways is highly dangerous. By studying the influence of the layout of the FGER on stress changes and energy accumulation within the upper pre-set coal roadway, the spatial layer layout of the FGER is optimized to avoid large stress concentrations in the upper pre-set coal roadway. From the initial roadway design to reduce the elastic strain energy accumulated before the coal roadway excavation, minimizing the possibility of coal and gas outbursts. Furthermore, reducing the internal energy of coal gas and enabling full utilization of the

FGER in the anti-outburst system of coal roadway excavation can be achieved by implementing subsequent measures such as crossing boreholes for gas extraction and hydraulic punching.

According to the conservation of outburst energy in the process of coal road excavation, the effective accumulation of a large amount of elastic strain energy is the basis for dynamic disasters. The energy required to break the coal body and throw out the broken coal and other energy dissipation mainly comes from the gas expansion energy and the elastic strain energy of the coal body accumulated from the coal seam for a long time (Lin et al. 2010). In the outburst excitation stage, the energy of the broken coal body primarily comes from the release of strain energy of the coal body. At this time, the further expansion of a large amount of gas resolved by coal body crushing is the dominant energy source for subsequent outbursts. Therefore, the magnitude of the released strain energy determines the degree of broken coal body and the size of gas expansion energy (Yang et al. 2018; Díaz Aguado María and González 2007).

The unloading elastic modulus E_i and Poisson’s ratio ν after the coal body is damaged under principal stress mainly affects the release and accumulation of strain energy. When the coal and rock mass is undamaged, the strain energy density can be expressed as (Xie et al. 2005; Xiao et al. 2021; Zhang et al. 2018):

$$U^e = \frac{1}{2} \sigma_i \epsilon_i^e = \frac{1}{2} \sigma_1 \epsilon_1^e + \frac{1}{2} \sigma_2 \epsilon_2^e + \frac{1}{2} \sigma_3 \epsilon_3^e = \frac{1}{2} \left\{ \frac{\sigma_1^2}{E_1} + \frac{\sigma_2^2}{E_2} + \frac{\sigma_3^2}{E_3} - \nu \left[\left(\frac{1}{E_1} + \frac{1}{E_2} \right) \sigma_1 \sigma_2 + \left(\frac{1}{E_2} + \frac{1}{E_3} \right) \sigma_2 \sigma_3 + \left(\frac{1}{E_1} + \frac{1}{E_3} \right) \sigma_1 \sigma_3 \right] \right\} \quad (1)$$

Table 1 Mechanics parameters of rock formation

Lithology	Thickness (m)	Density (kg/m ³)	Bulk modulus (GPa)	Shear modulus (GPa)	Cohesion (MPa)	Tensile strength (MPa)	Internal friction angle (°)
Overlying rock	-	2500	6.67	4.00	4.2	3.1	29
Fine-grained sandstone-1	9	2550	4.10	2.58	4.5	3.9	30
Medium grained sandstone-1	9	2638	7.38	5.08	6.7	6.5	29
Siltstone	5	2529	3.14	1.98	2.9	3.2	28
Medium grained sandstone-2	10	2611	5.24	3.61	5.2	4.5	29
Mudstone	5	2403	3.57	1.74	1.7	1.2	25
Coal seam	5.6	1380	2.69	1.10	1.1	0.8	27
Fine-grained sandstone-2	5.4	2563	5.23	3.76	4.6	4	30
Marl-1	6	2488	3.48	1.80	2.8	6.2	28
Marl-2	3	2488	3.94	2.03	3.2	6.2	28
Limestone	12	2625	5.52	4.49	7.2	7.6	25
Bottom rock	-	2500	6.67	4.00	4.2	3.1	29

where, U^e is the strain energy density (MJ/m³), the elastic strain energy that can be released per unit volume of coal rock body, σ_i is the principal stress component, ε_i^e is the total elastic strain in the direction of the principal stress components, E_i is the unloading elastic modulus of coal rock body (MPa), and ν is the Poisson's ratio of coal body.

The conventional damage variable ω_i is introduced to represent the effect of coal body damage on the unloading modulus of elasticity E_i of the coal body.

$$E_i = (1 - \omega_i)E_0 \tag{2}$$

Where, E_0 is the initial modulus of elasticity (MPa) of the coal body without damage and substituting Eq. (2) into Eq. (1) can be obtained:

$$U^e = \frac{1}{2} \sigma_i \varepsilon_i^e = \frac{1}{2E_0} \left\{ \frac{\sigma_1^2}{1-\omega_1} + \frac{\sigma_2^2}{1-\omega_2} + \frac{\sigma_3^2}{1-\omega_3} - \nu \left[\left(\frac{1}{1-\omega_1} + \frac{1}{1-\omega_2} \right) \sigma_1 \sigma_2 + \left(\frac{1}{1-\omega_2} + \frac{1}{1-\omega_3} \right) \sigma_2 \sigma_3 + \left(\frac{1}{1-\omega_1} + \frac{1}{1-\omega_3} \right) \sigma_1 \sigma_3 \right] \right\} \tag{3}$$

Use the average values E' , ν' , ω' to represent E_0 and ν such that:

$$E' = (1 - \omega')E_0, \nu' = \frac{\nu}{1 - \omega'}, \omega' = \omega_i$$

Then the releasable elastic strain energy U^e can be expressed as:

$$U^e = \frac{1}{2E'} [\sigma_1^2 + \sigma_2^2 + \sigma_3^2 - 2\nu'(\sigma_1\sigma_2 + \sigma_2\sigma_3 + \sigma_1\sigma_3)] \tag{4}$$

For the convenience of calculation and engineering application, the initial modulus of elasticity E_0 and Poisson's ratio ν can be used directly, and Eq. (4) can be changed to:

$$U^e = \frac{1}{2E_0} [\sigma_1^2 + \sigma_2^2 + \sigma_3^2 - 2\nu(\sigma_1\sigma_2 + \sigma_2\sigma_3 + \sigma_1\sigma_3)] \tag{5}$$

The initial elastic modulus and Poisson's ratio of the coal body under different FGER layouts were constant values during this study. So the elastic strain energy U^e of per unit coal body is mainly determined by the principal stress components state of the coal body within the pre-set coal road range after the FGER excavation. The layout of the FGER can form a pressure relief zone on the upper part. Adjusting the layer layout of the FGER reduces the in situ stress in the pre-set coal roadway area, which can effectively reduce the elastic strain energy of coal accumulation, as shown in Fig. 2, and reduce the outburst risk of coal roadway excavation from the design. In Fig. 2, H_i is the depth of the corresponding rock layer

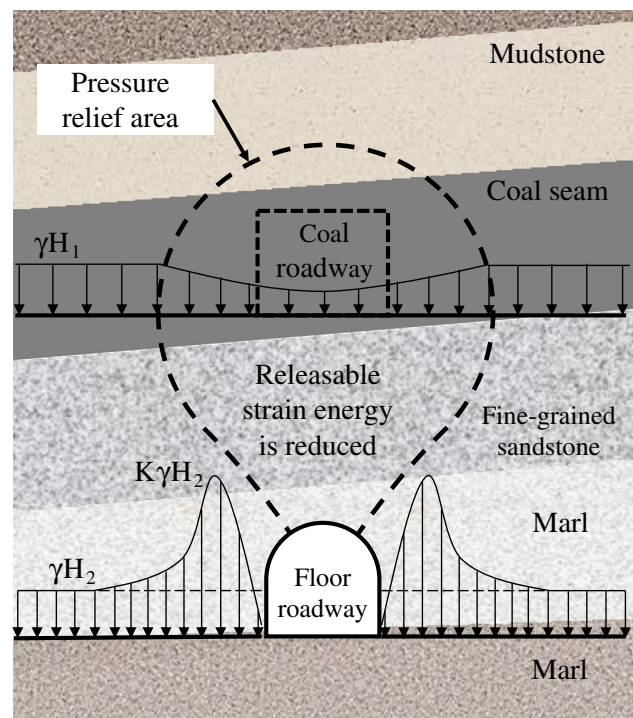


Fig. 2 Pressure relief and anti-outburst in the pre-set coal roadway area under the disturbance of the FGER excavation

from the surface, K is the peak stress coefficient, and γ is the capacitance.

Deformation coefficient and relative displacement

The authors used the deformation coefficient (K_h) to analyze the displacement and stability of the coal roadside after the pre-set coal roadway excavation, which is the ratio of the displacement of the coal roadway after the coal roadway excavation with and without the FGER. When $K_h < 1$, it means that the displacement of the roadside is smaller than the displacement of the roadside without a FGER, and the current layout of the FGER can improve the stability of the upper coal roadway. $K_h = 0.95$ was used as the evaluation standard during the project site implementation. With K_h as the model analysis indicator, it is possible to compare the damage to the roadway between various FGER layout methods and the damage of the roadway with and without the FGER.

After the coal seam mining, the FGER will move up with the coal seam floor as a whole. At this time, the deformation amount of individual roadsides cannot clearly express the damage to the roadway. The analysis of the relative distance of the roadway surroundings can effectively avoid the analysis error caused by the overall rise of the FGER.

Plastic zone distribution and coal seam floor damage mechanism

To study the influence of coal seam mining on the stability of the FGER, the authors simulated and analyzed the stress distribution of the coal seam floor after coal seam mining by the Mohr-Coulomb model. The failure state of any point of the coal seam floor could be judged by the distribution of the plastic zone from the numerical simulation.

According to the Coulomb strength criterion, the shear failure of a coal body along a certain structural plane needs to meet:

$$|\tau| = f\sigma + c = \sigma \tan \varphi + c \tag{6}$$

where, τ and σ are the shear and normal stresses on this structural surface, respectively, f is the coefficient of internal friction, c is the cohesive force on the structural surface, and φ is the angle of internal friction on the structural surface.

τ and σ can be expressed in terms of principal stresses $\sigma_1, \sigma_2, \sigma_3$ according to the Mohr stress circle:

$$\sigma = \frac{1}{2}(\sigma_1 + \sigma_3) + \frac{1}{2}(\sigma_1 - \sigma_3) \cos 2\theta \tag{7}$$

$$\tau = \frac{1}{2}(\sigma_1 - \sigma_3) \sin 2\theta \tag{8}$$

where, θ is the angle between the structural plane and the minimum principal stress σ_3 and $\theta = (\pi + 2\varphi)/4$.

Substituting Eqs. (7) and (8) into Eq. (6):

$$|\tau| - f\sigma = c = \frac{1}{2}(\sigma_1 - \sigma_3)(\sin 2\theta - f \cos 2\theta) - \frac{1}{2}f(\sigma_1 + \sigma_3) \tag{9}$$

The derivative of Eq. (9) concerning θ yields the extreme value $\tan 2\theta = -1/f$, and $2\theta \in (\pi/2, \pi)$, substituting Eq. (10) into Eq. (9) to obtain the maximum value of $|\tau| - f\sigma$ as shown in Eq. (11).

$$\begin{cases} \sin 2\theta = \frac{1}{\sqrt{f^2+1}} \\ \cos 2\theta = -\frac{f}{\sqrt{f^2+1}} \end{cases} \tag{10}$$

$$\{|\tau| - f\sigma\}_{\max} = \frac{1}{2}(\sigma_1 - \sigma_3)\sqrt{f^2 + 1} - \frac{1}{2}f(\sigma_1 + \sigma_3) \tag{11}$$

According to Eq. (6), when Eq. (11) $\geq c$, the coal body will be damaged, and if Eq. (11) $< c$, the coal body will not be damaged.

Numerical simulation I: analysis of the stability of roadway excavation before coal seam mining

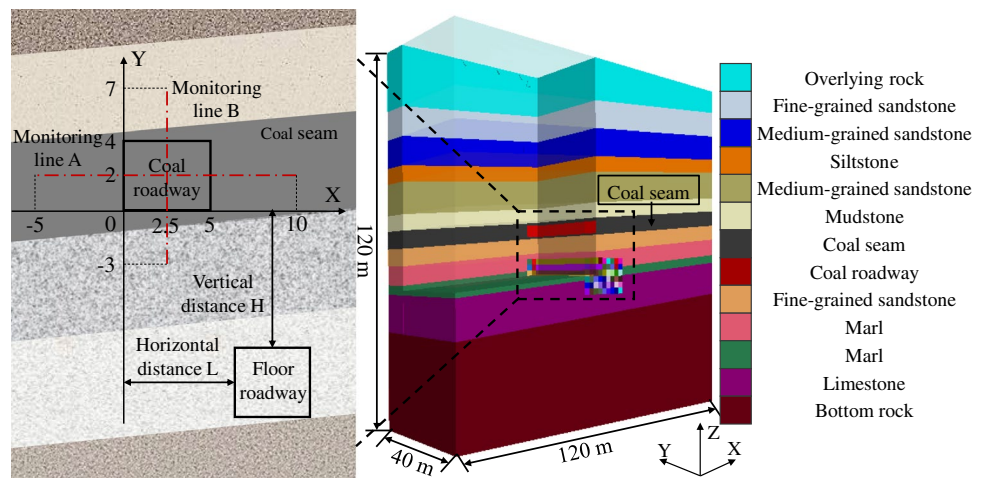
Model I establishment

A numerical model containing 13 coal seams was established according to the actual stratigraphic distribution characteristics, as shown in Fig. 3. The corresponding normal phase displacements were constrained on the four sides of the model, and the three-dimensional displacements were constrained at the bottom of the model. The design size was 120 m \times 120 m \times 40 m to prevent the influence of model boundary effects. The FGER (4 m \times 4 m) was excavated 30 m along the coordinate y-axis, and the coal roadway (5 m \times 4 m) was excavated 20 m along the y-axis, with a step length of 5 m.

Numerical simulation I scheme

According to the previous construction experience of the Shoushan mine, the FGER was generally selected within 8~20 m below the floor and 0~15 m horizontal distance from the coal roadway. This range was taken as the permissible range for the layout in this research. From Table 1, it is clear

Fig. 3 Numerical simulation I model



that the acceptable layout range of the FGER is marl or limestone. The allowable vertical distance (H) was divided into six parts, with 2 m as the interval; the horizontal distance (L) was 0~18 m, with 2 m as the interval. Different H and L are combined, as shown in Fig. 3, to form the simulation schemes as shown in Table 2. Horizontal measuring line A and vertical measuring line B were arranged in the pre-set roadway section to monitor stress distribution changes, as shown in Fig. 3.

Analysis of simulation I results

(1) The impact of FGER excavation on the elastic potential accumulation of the pre-set coal roadway Under the influence of the FGER excavation, the ground stress will be redistributed and form a stress concentration area and pressure relief area within the range of pre-set coal roadway. The elastic strain energy U^e of per unit volume of coal body is mainly determined by the principal stress components state of the coal body within the pre-set coal road range after the FGER excavation. The average unit volume elastic strain energy of the coal accumulated of the pre-set coal roadway was calculated according to Eq. (5), as shown in Fig. 4. “Initial” is the elastic strain energy U^e_i in the per unit volume of original coal without FGER. The average of “Initial” is 202.2 KJ, which was used as the standard to judge the influence of each layout method on the elastic strain energy of coal accumulated in the pre-set coal roadway. When the L is 0~2 m, the elastic strain energy accumulated of the unit coal body is almost equal in the same H. When the L is more than 2 m, the accumulated elastic strain energy also increases with the increase of L. The smaller the H, the greater the increased rate of elastic strain energy accumulated in the unit coal. Among the 40 layout options, only three layout methods of FGER (H8L12, H8L14, H10L14) accumulate elastic strain energy greater than U^e_i . The rest of the layout methods can reduce the elastic strain energy accumulated in the original coal. When the L is greater than 12 m, the elastic strain energy collected in the unit volume of the coal body of the pre-set coal roadway is almost equal to the amount

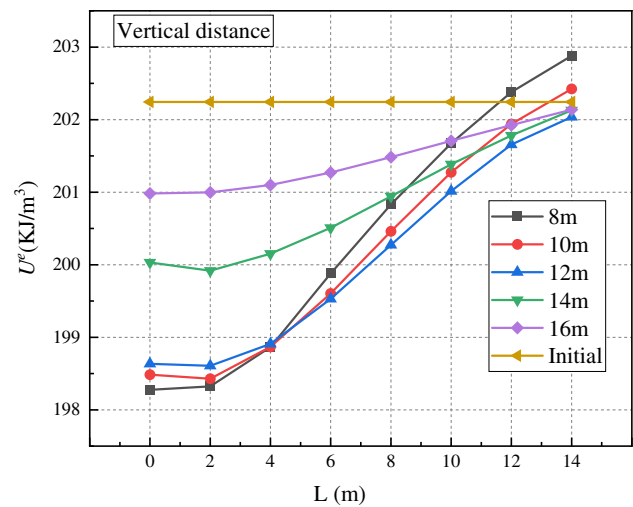


Fig. 4 Elastic strain energy of coal body in the range of pre-set coal roadway under different layout schemes

of the elastic strain energy accumulated without FGER. It indicates that when the L is more than 12 m, the excavation of the FGER has less or almost no effect on the upper pre-set coal roadway and cannot effectively reduce the elastic strain energy accumulated in the unit volume of the coal. Therefore, when H and L are greater than a fixed value, the FGER cannot play the role of pressure relief and anti-outburst. With the L and H decrease between the FGER and the upper pre-set coal roadway, the more pronounced the pressure relief of the coal body of the pre-set coal roadway, the smaller the elastic strain energy accumulated in the unit volume of coal. Among them, the pressure relief effect is best when the H is 8~12 m, and the L is 0~4 m, the elastic strain energy accumulated in the unit volume of coal is smaller, the effect of anti-outburst is better.

(2) Displacement of coal roadsides after coal roadway excavation Based on the simulation results, the average displacement of the roadway’s floor, roof, and two roadsides after coal roadway excavation is 0.05 m, 0.1 m, and

Table 2 Numerical simulation scheme

Simulation scheme (1~40)	Vertical distance H (m)							
	8	10	12	14	16			
Horizontal distance L (m)	0	2	4	6	8	10	12	14
	1: H8L0	2: H8L2	3: H8L4	4: H8L6	5: H8L8	6: H8L10	7: H8L12	8: H8L14
	9: H10L0	10: H10L2	11: H10L4	12: H10L6	13: H10L8	14: H10L10	15: H10L12	16: H10L14
	17: H12L0	18: H12L2	19: H12L4	20: H12L6	21: H12L8	22: H12L10	23: H12L12	24: H12L14
	25: H14L0	26: H14L2	27: H14L4	28: H14L6	29: H14L8	30: H14L10	31: H14L12	32: H14L14
	33: H16L0	34: H16L2	35: H16L4	36: H16L6	37: H16L8	38: H16L10	39: H16L12	40: H16L14

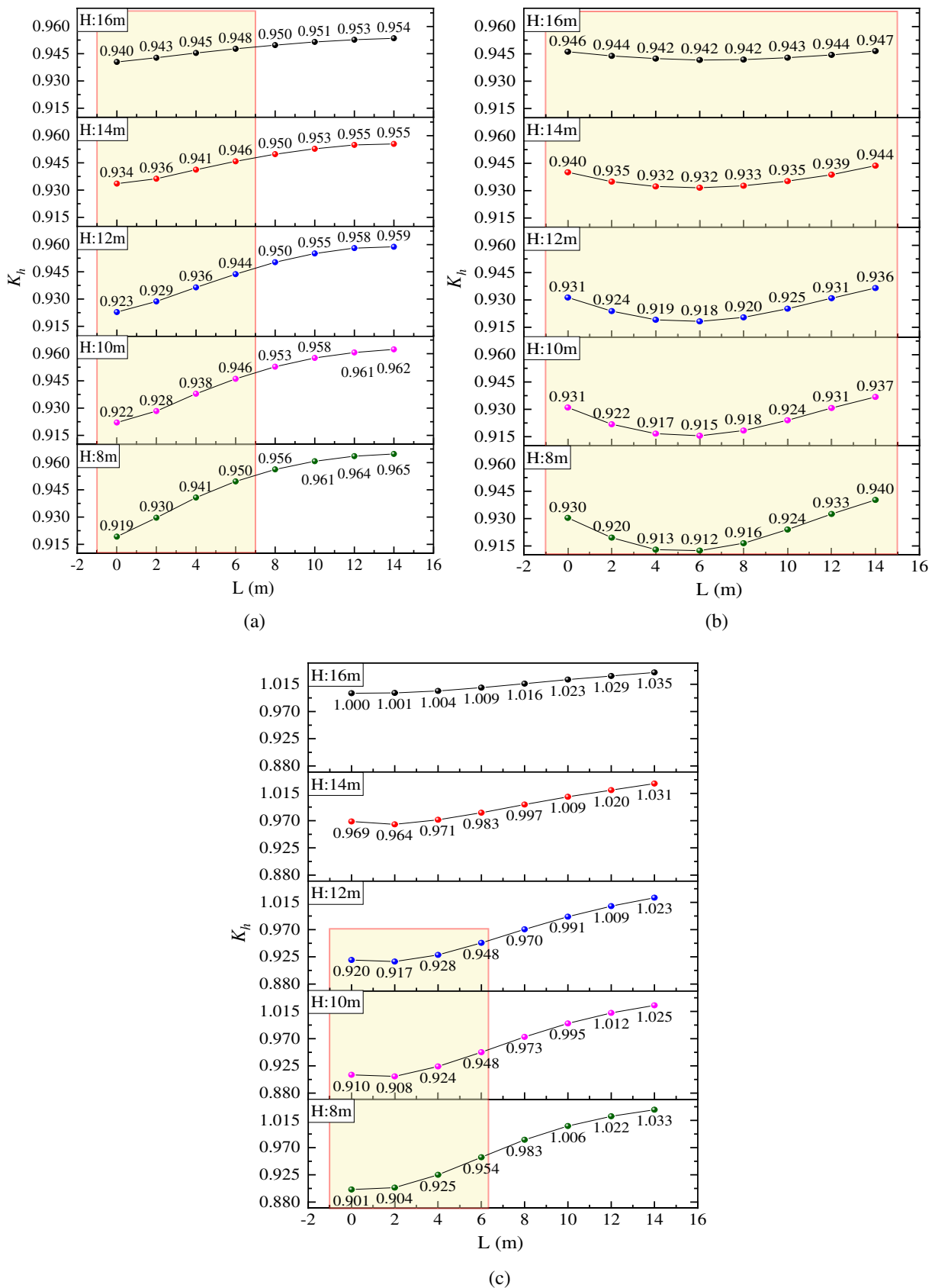


Fig. 5 K_h of the coal roadway. **a** Upper roadside, **b** lower roadside, and **c** the floor

0.11 m, respectively. The K_h of the two sides is less than 1, as shown in Fig. 5. All layouts of the FGER can reduce the strain on the coal roadside and improve the stability of the upper coal roadway within the L of 0~14 m and the H of 8~16 m. According to the K_h of the surrounding rock of the coal roadway under different layouts of the FGER, when the H is 16 m, the FGER has less influence on the deformation of the coal roadway. The FGER and coal roadway are relatively independent and have a more negligible effect on each other. However, at this time, the FGER also cannot play a role in releasing the elastic strain energy of the upper pre-set coal roadway and its surrounding coal body.

The K_h of coal roadsides is shown in Fig. 5a and b. When the H is 8~16 m, with the increase of H, the pressure relief effect of coal roadway by the FGER gradually decreases, the K_h of coal roadsides increases, and the deformation of roadsides increases slowly close to the deformation of roadsides without an FGER. When the L is 0~14 m, the pressure relief area formed by the FGER is gradually far away from the lower coal roadside with the increase of L. The deformation of the lower roadside of the coal roadway is the smallest when the L is 0 m, which will gradually increase with the increase of L. Due to the width of the coal roadway being 5 m, when the L is 4~6 m, the upper coal roadside is in the pressure relief area formed by the FGER, and the deformation of the upper roadside of the coal roadway is the smallest. The pressure relief zone created by the FGER can relieve the pressure of the upper coal roadway and improve the stability of the coal roadsides. When the H is 8~16 m, and the L is 0~6 m, the K_h of the lower coal roadside is less than 0.95. When the H is 8~16 m, and the L is 0~14 m, the K_h of the upper coal roadside is less than 0.95.

The pressure relief area formed by the FGER has less influence on the roof. The distribution of the K_h curve is approximately horizontal under the condition of a certain H. With the increase of H, the sinking amount of the roof gradually decreases. The displacement of the coal roadway floor is shown in Fig. 5c. When the L is 0~5 m, the pressure relief area formed by the FGER is located below the coal roadway, which can effectively improve the stability of the coal roadway floor and reduce the amount of floor heave. When the H and L increase, the K_h of coal roadway floor increases, the floor heave of coal roadway increases, and the stability decreases. When the H is 8~12 m and the L is 0~5 m, the K_h of the coal roadway floor is less than 0.95.

In the pre-set layout range of FGER (H: 8~16 m, L: 0~14 m), when the L is 0~6 m, the K_h of coal roadsides is less than 0.95. The layout of the FGER in this range can improve the stability of the surrounding rock of the upper coal roadsides,

and the K_h of the coal roadway roof of all layout methods is greater than 0.95.

Numerical simulation II: the failure and the stability of the FGER under the influence of mining

Model II description and simulation scheme

A numerical model containing 13 coal seams was established according to the stratigraphic distribution characteristics shown in Fig. 6. The model size was 400 m × 400 m × 200 m to prevent the influence of model boundary effects. The FGER (4 m × 4 m) was excavated in the direction of the coordinate y-axis from y = 100 to y = 350 m, a total of 250 m, with a step length of 25 m. The coal seam was mined in the direction of the coordinate y-axis from y = 100 to y = 300 m, a total of 200 m, with a step length of 25 m.

The numerical simulation consists of two parts, and the first part analyzed the damage to the coal seam floor affected by mining in the case without FGER. The second part explored the impact of coal seam mining on the stability of the surrounding rock of the FGER.

Analysis of simulation II results

(1) The plastic zone distribution of the floor under the influence of mining The plastic zone of the floor behind the coal mining face from 0 to 50 m after coal mining is shown in Fig. 7. Since using the Mohr-Coulomb model, the authors could analyze the damaged area of the coal seam floor according to the plastic zone calculated with the Mohr-Coulomb criterion in Eq. (11).

Under the coal mining face directly, the floor has not been destroyed within the L of 0~4 m and the H of 14~18 m from the coal roadway, and the damage depth of the coal seam floor is the smallest. Under pressure redistribution affected by mining, there will be a pressure relief zone under the mined-out area, while the supporting pressure zone will appear below the coal pillar. Due to the floor stress being closest to the original rock stress, the floor is more stable directly below the two ends of the working face. As the working face moves forward, there is a “sharp increase - sharp decrease - return to original rock stress” in the floor, forming rock compression, expansion, and compaction zones. In the range from 10 m in front to 50 m behind the coal mining working face, the coal seam floor is gradually destroyed due to compression and expansion. When it is located 30 m behind the coal mining face, the proposed layout range of the FGER has been completely destroyed. According to the distribution of the plastic zone of the floor after coal seam mining, the FGER is less affected by coal seam mining when it is arranged directly below the coal roadway.

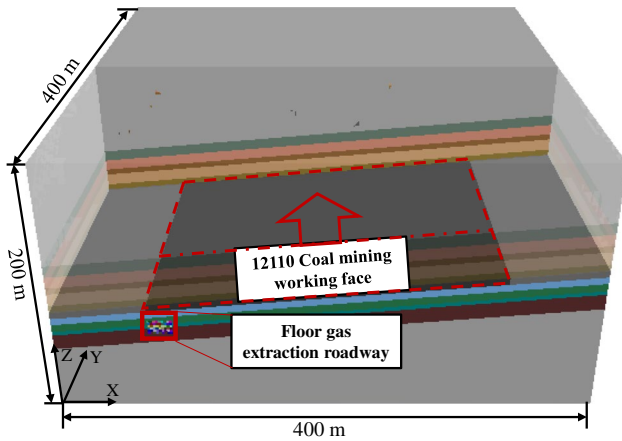


Fig. 6 Numerical simulation II model

(2) **The displacement of the surrounding rock in the FGER under the influence of mining** Figure 8 shows the relative displacement of the surrounding rock of the FGER after being affected by coal seam mining. All deformations were derived from the cross-measurement points of the roadway. Before being affected by coal seam mining, the deformation of the upper roadside and the lower roadside of the FGER is approximately equal. Under the influence of the model stratigraphic parameters setting, the roadside measurement point is in marl when the H is 8~12 m, and the deformation is about 0.033 m. When the H is 14~16 m, the roadside measurement point is in limestone, the roadside is stable, and the displacement is about 0.01 m.

After being affected by coal seam mining, the displacement of the surrounding rock of the FGER becomes larger. The upper roadside of the FGER is in the pressure relief zone of the coal mined-out area, and the lower roadside is in the original rock stress zone of the coal pillar side, so the displacement of the upper roadside of the FGER is smaller

Fig. 7 Distribution of the plastic zone of the floor 0~50 m behind the coal mining face

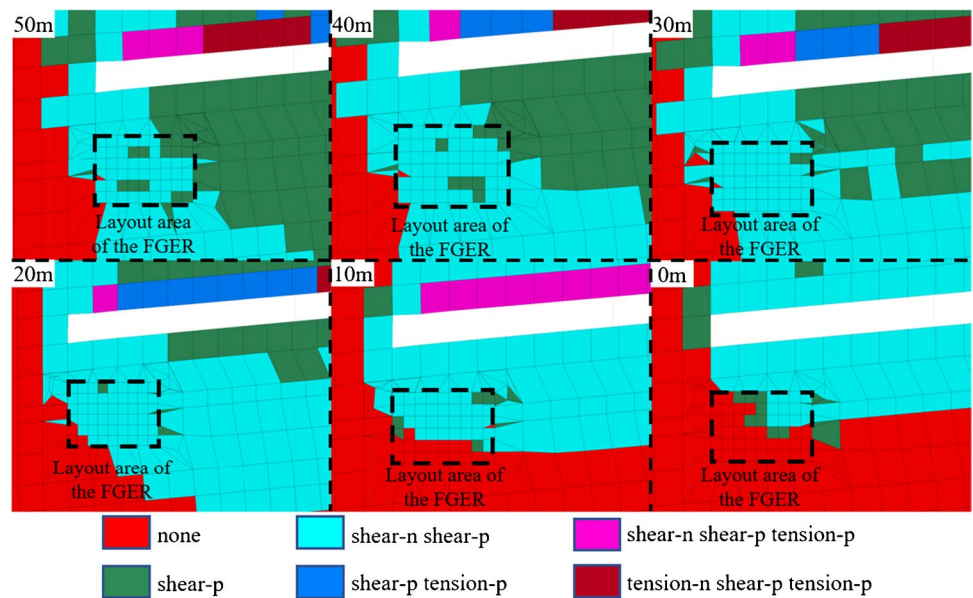
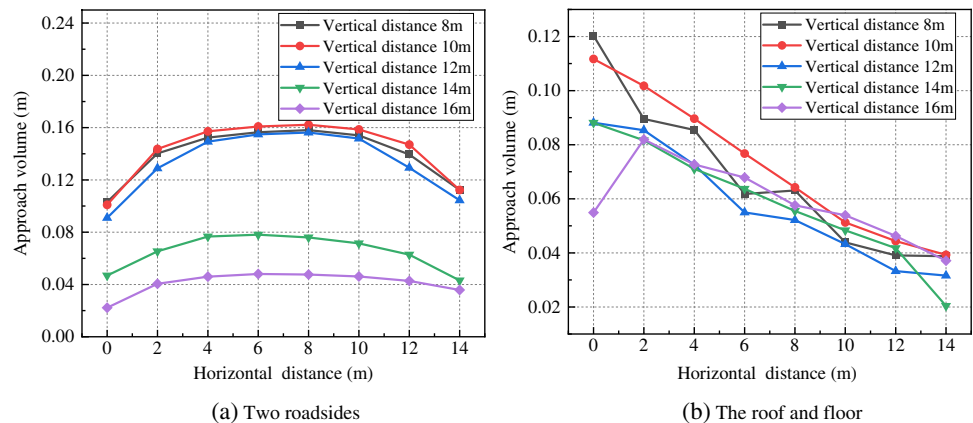


Fig. 8 Relative displacement of the surrounding rock of the FGER before and after being affected by mining. a Two road-sides and b the roof and floor



than that of the lower roadside. When the H is 8~12 m, the two roadsides measurement points of the FGER are in the marl. The upper roadside deformation is similar to about 0.05~0.07 m, and the lower roadside deformation is about 0.08~0.1 m. The upper roadside deformation is the smallest when the H is 8 m. When the H is 14 and 16 m, the displacement is small because the two roadsides measurement points of the FGER are in the marl, the upper roadside displacement is about 0.03 and 0.015 m, and the lower roadside displacement is about 0.4 and 0.3 m, respectively. Compared with before being affected by mining, the incremental displacement of the surrounding rock in the lower roadside of the FGER is about twice the incremental displacement of the upper roadside. With the increase of the L between the FGER and the upper coal roadway, the displacement and relative displacement of two roadsides increase first and then decrease. This phenomenon may be due to the sharp change of the vertical stress curve below the two ends of the working face, and the FGER also transitions from the approximate original rock stress zone to the pressure relief zone. When the L is 0, 2, 12, and 14 m, the vertical stress within the range of the FGER is relatively stable, and the relative displacement of the roadsides is small; when the L is 4, 6, 8, and 10 m, the vertical stress within the range of the FGER has a significant difference in tendency, and the relative displacement of the roadsides is large.

As the FGER was layout below the end of the working face, the displacement variation is similar to the vertical stress variation, which change significantly along with the coal seam tendency. The FGER roof and floor displacement increase with L increasing and H decreasing. When the L is 0 m or the H is 16 m, the deformation is relatively small. From the displacement of the roof and floor, we could find that the FGER moves up as a whole with the occurrence of the floor heave in the coal mined-out area. As shown in Fig. 8b, the relative displacement of the roof and floor decreases with the increase of the L between the FGER and the upper coal roadway, and the growth of the H has less influence on the relative displacement of the roof and floor.

The reasonable layer layout of the FGER and engineering application

Simulation results

During the simulation process, within the layout range of the pre-set coal roadway, the authors set up 40 simulation scenarios at 2 m intervals. With the decrease of the L and H between the FGER and the upper pre-set coal roadway, the more pronounced the pressure relief of the coal body of the pre-set coal roadway, and the elastic strain energy

accumulated in the unit volume of coal become smaller. Among them, the pressure relief effect is best when the H is 8~12 m, and the L is 0~4 m, the elastic strain energy accumulated in the unit volume of coal is smaller, the effect of anti-outburst is better than other layouts. When the L is 0~6 m, the K_h of coal roadsides is less than 0.95. The layout of the FGER in this range can improve the stability of the surrounding rock of the upper coal roadsides. The FGER is less affected by coal seam mining when arranged directly below the coal roadway with working face advancement. When the L is 0, 2, 12, and 14 m, the vertical stress within the range of the pre-set FGER is relatively stable, and the relative displacement of the roadsides is small after excavation. With the increase of the L, the relative displacement of the roof and floor decreases. And the growth of the H has less influence on the relative displacement of the roof and floor. According to the simulation results, the best layout range is 8~12 m of H and 0~2 m of L. Also, according to the actual situation, the FGER could be layout in the range of 8~12 m of H and 2~6 m of L.

Lithology analysis of coal seam floor

The direct floor of 12,110 working face is sandstone and mudstone intercalated, which is 4.2~5.8 m. Below sandstone and mudstone intercalated are marl and limestone, the thickness is 12~17 m, and the average thickness is 15.5 m. The upper part is marl; the lower part is limestone, intercalated mudstone, and the rock solidity coefficient is $f = 6\sim 8$. A coal line is used as the 16~17 coal seam marker layer at the 8~12 m away from the 15~17 coal seam floor, with an average thickness of 0.3 m. Considering the excavation speed and rock solidity coefficient of the FGER in different rock strata, the FGER could be arranged in marl and above the limestone, and the coal line could be used as a reference when excavating.

Analysis of drilling efficiency and extraction effect

The previous construction experience of the Shoushan mine shows that when the horizontal distance between the FGER and upper coal roadway is 6 m, the FGER and upper coal roadway are relatively stable. When the horizontal distance between the FGER and upper coal road of 12,110 working face is 6 m, it can effectively avoid encountering bad geological conditions such as faults during the excavation process. Therefore, the final L between the FGER of the mechanical transportation roadway and the mechanical transportation roadway is set at 6 m. A total of 12,110 working face has 239 groups of crossing boreholes, each group has 12 boreholes and a deep borehole, and the distance between borehole groups is 6.4 m. The specific borehole arrangement is shown

Fig. 9 The arrangement of a group of crossing boreholes

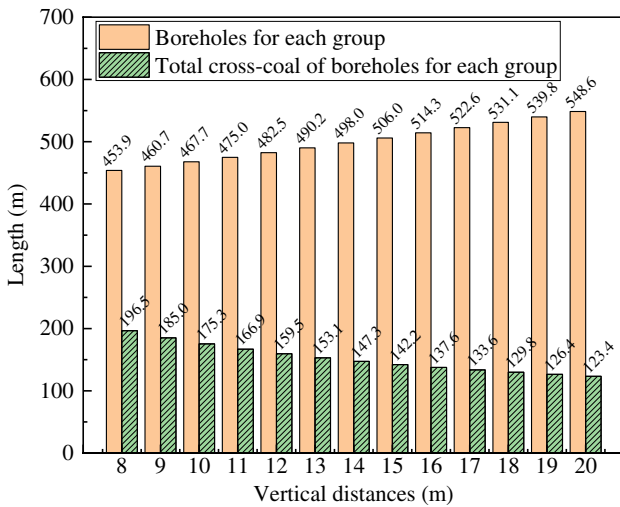
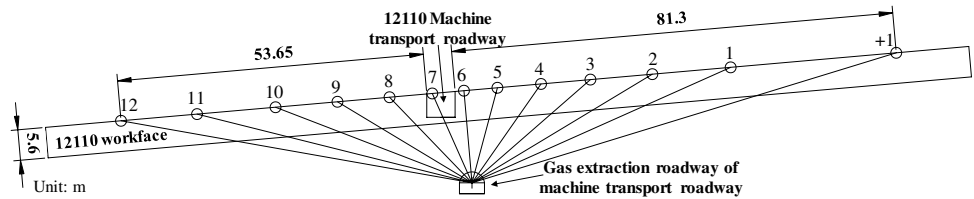


Fig. 10 Total length of boreholes and cross-coal for each group

in Fig. 9. Each group of boreholes controls the coal body area within 130 m of the mechanical transportation roadway.

The total length of boreholes and the cross-coal length for a horizontal distance of 6 m and a vertical distance of 8~20 m, respectively, were calculated in Fig. 10. In the range of 8~16 m of H, each additional 1 m of H will increase the total length of each group of boreholes by 6~9 m and add the construction cost by US \$65~100. The total length of each group of boreholes with 16 m of H is increased by about 94.7 m compared with the whole length of boreholes with 8 m of H, and the total increase of 239 groups is 22,633.3 m. According to the maximum speed of mining drilling machine ZDY4000R 1.5 m/min, the drilling time of each floor extraction roadway at 16 m of H is 250 h longer than that at 8 m of H, and the construction cost increases by US \$250,000. After the crossing boreholes constructing, the hydraulic punching operation starts. During the study, the cavity formed by hydraulic punching is generally assumed to be cylindrical, releasing the coal stress and gas pressure in advance and providing enough space for coal expansion and deformation. The amount of coal output per meter from the hydraulic punching borehole of the FGER is about 0.53 t. The longest total cross-coal length of each group of boreholes is 196.5 m when the vertical distance is 8 m. Increasing the cross-coal length of the boreholes can increase the amount of total coal output. And the volume of the hydraulic

punching cavity also increases so that the surrounding coal body can be fully expanded and deformed to improve the porosity of the surrounding coal body and increase the gas extraction concentration and gas extraction amount.

When the H between the FGER and the mechanical transportation roadway is 8 m, it can effectively reduce the total construction length of each group of boreholes, save drilling time, reduce the construction cost of the boreholes, increase the total cross-coal length and the amount of coal output, improve the construction efficiency and utilization rate of the penetration borehole, increase the porosity of the coal body around the borehole, and improve the gas extraction concentration and gas extraction amount.

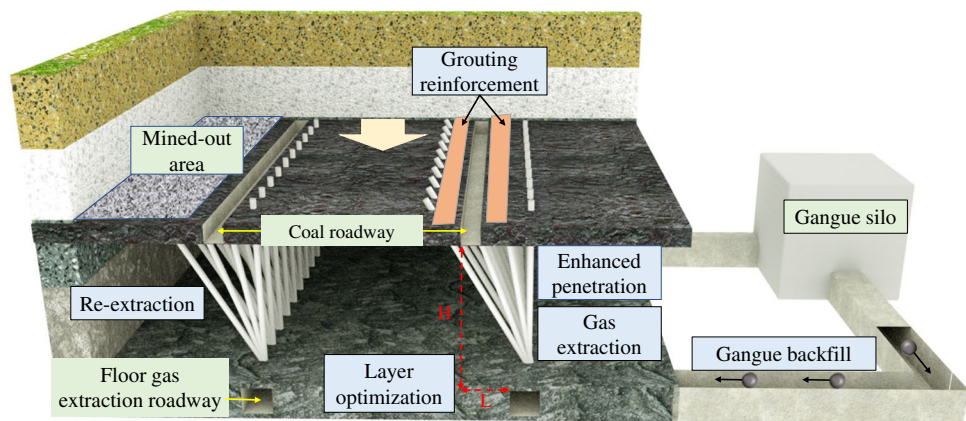
Layout of the floor gas extraction roadway

Based on the simulation analysis of the state of coal, gas outbursts of energy accumulated in coal roadway and the FGER stability under the influence of mining and combined coal seam floor lithology, drilling efficiency, and extraction effect under the different layouts of FGER. The authors proposed a comprehensive evaluation system with four aspects “anti-burst, stability, lithology, and extraction.” The FGER of the mechanical transport roadway would be arranged in the marl within the L of 6 m and H of 8~12 m from the mechanical transport roadway. The coal line at 8~12 m below the 15–17 coal seam floor would be regarded as the marker line. The roof of the FGER will excavate about 1.5 m above the coal line.

Discussion

The stability of the FGER is the result of the joint influence of many factors. At present, there is no complete system to analyze the layer layout of the FGER or other roadways. In this paper, the authors analyzed the layout optimization and utilization of the FGER from the four aspects of “anti-outburst, stability, lithology, and extraction” and considered the whole cycle of roadway excavation to coal seam mining. However, there are still some limitations, such as not considering the energy accumulation of the roadway excavation working face and the geohydrological state. The research idea of this paper can provide a reference for the layer layout of the FGER, which no longer only analyzes FGER but establishes a connection

Fig. 11 The full life cycle utilization of gas extraction roadway at the floor of the outburst coal seam



with other research objects, such as coal roadway excavation, coal seam mining, gas control, and utilization. Regional overall pressure relief is currently the primary way to solve the gas extraction problem during the mining process of high gas and low permeability prominent coal seam. As the main body of the regional overall pressure relief, the layer layout and utilization of the FGER have essential significance for safe mining and methane control.

In response to the above problems, the authors proposed comprehensive gas management based on the whole life cycle of the FGER. The layout of the FGER and the coal mining system, coal seam weakening and reinforcement system, gas extraction system, and gangue filling system are studied as a whole, as shown in Fig. 11. Exploring the full time-space gas extraction technology model and the integrated technology system of “Layer optimization, Enhanced penetration, Grouting reinforcement, Gas extraction, Gangue backfill” for the FGER of the outburst coal seam will be the focus of later research.

Conclusions

- (1) Adjust the layer layout of the FGER to ensure that the pre-set coal roadway is located in the pressure relief zone formed after stress redistribution, which can effectively unload the coal body within the pre-set coal roadway and reduce the elastic strain energy of coal accumulation. At the same time, the upper coal tunnel strip area is pre-extracted with the crossing boreholes to reduce the gas pressure in the coal body to prevent coal and gas outbursts during the coal roadway excavation process.
- (2) According to the field pictures taken in the FGER and the distribution of plastic zone formed by numerical simulation, both show that the stability of the FGER will be strongly affected by the coal seam mining. When arranged directly below the coal roadway, the FGER is less affected by the coal seam mining.

- (3) When the vertical distance between the FGER and mechanical transportation roadway reduces, the total construction length of each group of crossing boreholes could decline. The whole length of the cross-coal and the amount of hydraulic punching out of coal increase to effectively improve the construction efficiency and utilization rate of the crossing borehole and increase the gas extraction concentration and gas extraction volume.
- (4) According to the numerical simulation and industrial experiments, a comprehensive evaluation system for selecting the reasonable FGER layout based on the four aspects of “anti-outburst, stability, lithology, and extraction” was formed, which will provide a reference for other similar coal mine projects.

Funding This work was financially supported by the National Science Fund for Distinguished Young Scholars (51925404), the National Natural Science Foundation of China (51774278, 52104228), and the China Postdoctoral Science Foundation (2021M693409).

Declarations

Conflict of interest The authors declare that they have no competing interests.

References

- Black DJ (2019) Review of coal and gas outburst in Australian underground coal mines. *Int J Min Sci Technol* 29(6):815–824
- Díaz Aguado María B, González NC (2007) Control and prevention of gas outbursts in coal mines, Riosa–Olloniego coalfield, Spain. *Int J Coal Geol* 69(4):253–266
- Guo XF, Li YE, Zhou GD, He ZJ, Yu HR, Xu YC, Xiong F (2021) Stability analysis and reasonable layout of floor drainage roadway above confined water and under mining influence. *Geofluids* 2021:1–11
- Jeon S, Jongwoo K, Youngho S, Changwoo H (2004) Effect of a fault and weak plane on the stability of a tunnel in rock-a-scaled

- model test and numerical analysis. *Int J Rock Mech Min Sci* 41(3):658–663
- Jiang LS, Atsushi S, Mitri HS, Nianjie M, Hongtao L, Zhen H (2016) Influence of fracture-induced weakening on coal mine gateroad stability. *Int J Rock Mech Min Sci* 88:307–317
- Jing HW, Wu JY, Yin Q, Wang K (2020) Deformation and failure characteristics of anchorage structure of surrounding rock in deep roadway. *Int J Min Sci Technol* 30(5):593–604
- Karacan CÖ, Ruiz FA, Michael C, Sally P (2011) Coal mine methane: a review of capture and utilization practices with benefits to mining safety and to greenhouse gas reduction. *Int J Coal Geol* 86(2-3):121–156
- Lee Y-Z, Wulf S (2008) Determination of the round length for tunnel excavation in weak rock. *Tunn Undergr Space Technol* 23(3):221–231
- Lei Y, Cheng YP, Ren T, Tu QY, Shu LY, Li YX (2020) The energy principle of coal and gas outbursts: experimentally evaluating the role of gas desorption. *Rock Mech Rock Eng* 54(1):11–30
- Li J (2020) The coal pillar design method for a deep mining roadway based on the shape of the plastic zone in surrounding rocks. *Arab J Geosci* 13(12):1–12
- Li Y, Ma N, Ma J (2018) Surrounding rock's failure characteristic and rational location of floor gas drainage roadway abovedeep confined water. *J China Coal Soc* 43:2491–2500
- Li H, Ma JK, Wang ZQ, Wang W, Liu YW (2020a) A gas outburst prevention and control strategy for single thick coal seams with high outburst risk: a case study of Hudi Coal Mine in Qinshui Basin. *Energy Sci Eng* 8(7):2471–2491
- Li C, Wu Z, Zhang W, Sun Y, Zhu C, Zhang X (2020b) A case study on asymmetric deformation mechanism of the reserved roadway under mining influences and its control techniques. *Geomech Eng* 22:449–460
- Lin BQ, Zhai C, Zhu CJ (2010) Theory and technology of mine gas prevention and control. China University of Mining and Technology Press, Xuzhou
- Liu QL, Wang EY, Kong XG, Li Q, Hu SB, Li DX (2018) Numerical simulation on the coupling law of stress and gas pressure in the uncovering tectonic coal by cross-cut. *Int J Rock Mech Min Sci* 103:33–42
- Lu SQ, Cheng YP, Ma JM, Zhang YB (2014) Application of in-seam directional drilling technology for gas drainage with benefits to gas outburst control and greenhouse gas reductions in Daning coal mine, China. *Nat Hazards* 73(3):1419–1437
- Lu S, Chengfeng W, Qingquan L, Yongliang Z, Jie L, Zhanyou S, Liang W (2019) Numerical assessment of the energy instability of gas outburst of deformed and normal coal combinations during mining. *Process Saf Environ Prot* 132:351–366
- Małkowski P (2015) The impact of the physical model selection and rock mass stratification on the results of numerical calculations of the state of rock mass deformation around the roadways. *Tunn Undergr Space Technol* 50:365–375
- Mo S, Sheffield P, Corbett P, Ramandi HL, Oh J, Canbulat I, Saydam S (2020) A numerical investigation into floor buckling mechanisms in underground coal mine roadways. *Tunn Undergr Space Technol* 103:103497
- Moore TA (2012) Coalbed methane: a review. *Int J Coal Geol* 101:36–81
- Mu ZL, Liu GJ, Yang J, Zhao Q, Atif J, Gong SK, Cao JL (2019) Theoretical and numerical investigations of floor dynamic rupture: a case study in Zhaolou Coal Mine, China. *Saf Sci* 114:1–11
- Pan XK, Cheng H, Chen J, Zhou XP (2020) An experimental study of the mechanism of coal and gas outbursts in the tectonic regions. *Eng Geol* 279:105883
- Ranjith PG, Zhao J, Ju M, De Silva RV, Rathnaweera TD, Bandara AK (2017) Opportunities and challenges in deep mining: a brief review. *Engineering* 3(4):546–551
- Shen BT (2013) Coal mine roadway stability in soft rock: a case study. *Rock Mech Rock Eng* 47(6):2225–2238
- Si G, Cai W, Wang S, Li X (2020) Prediction of relatively high-energy seismic events using spatial–temporal parametrisation of mining-induced seismicity. *Rock Mech Rock Eng* 53(11):5111–5132
- Tang W, Zhai C, Xu JZ, Sun Y, Cong YZ, Zheng YF (2021) The influence of borehole arrangement of soundless cracking demolition agents (SCDAs) on weakening the hard rock. *Int J Min Sci Technol* 31(2):197–207
- Tsesarsky M, Erez G, Eli M (2013) 3-D global-local finite element analysis of shallow underground caverns in soft sedimentary rock. *Int J Rock Mech Min Sci* 57:89–99
- Tu Q, Cheng Y, Ren T, Wang Z, Lin J, Lei Y (2019) Role of tectonic coal in coal and gas outburst behavior during coal mining. *Rock Mech Rock Eng* 52(11):4619–4635
- Wang C, Wang Y, Lu S (2000) Deformational behaviour of roadways in soft rocks in underground coal mines and principles for stability control. *Int J Rock Mech Min Sci* 37(6):937–946
- Wang Q, Gao HK, Jiang B, Li SC, He MC, Qin Q (2021) In-situ test and bolt-grouting design evaluation method of underground engineering based on digital drilling. *Int J Rock Mech Min Sci* 138:104575
- Wei CC, Zhang CG, Ismet C, Huang WP (2021) Numerical investigation into impacts of major fault on coal burst in longwall mining - a case study. *Int J Rock Mech Min Sci* 147:104907
- Wu GJ, Chen WZ, Jia SP, Tan XJ, Zheng PQ, Tian HM, Rong C (2020) Deformation characteristics of a roadway in steeply inclined formations and its improved support. *Int J Rock Mech Min Sci* 130:104324
- Xiao WJ, Yu G, Li HT, Zhan WY, Zhang DM (2021) Experimental study on the failure process of sandstone subjected to cyclic loading and unloading after high temperature treatment. *Eng Geol* 293:106305
- Xie HP, Ju Y, Li LY (2005) Criteria for strength and structural failure of rocks based on energy dissipation and energy release principles. *Chin J Rock Mech Eng* 24(17):3003–3010
- Xue Y, Gao F, Liu XG, Liang X (2017) Permeability and pressure distribution characteristics of the roadway surrounding rock in the damaged zone of an excavation. *Int J Min Sci Technol* 27(2):211–219
- Yang SQ, Chen M, Jing HW, Chen KF, Meng B (2017) A case study on large deformation failure mechanism of deep soft rock roadway in Xin'an coal mine, China. *Eng Geol* 217:89–101
- Yang W, Wang H, Lin BQ, Wang YK, Mao XB, Zhang JG, Lu YC, Wang M (2018) Outburst mechanism of tunnelling through coal seams and the safety strategy by using “strong-weak” coupling circle-layers. *Tunn Undergr Space Technol* 74:107–118
- Yu BH, Cheng JW, Yang SQ, Wang DM (2014) Characterizing dilatation energy of released gas from underground coal seam by drilling boreholes. *Nat Hazards* 75(3):2965–2984
- Yu X, Xu LC, Regenauer-Lieb K, Jing Y, Tian FB (2020) Modeling the effects of gas slippage, cleat network topology and scale dependence of gas transport in coal seam gas reservoirs. *Fuel* 264:116715
- Zhang ZP, Xie HP, Zhang R, Zhang ZT, Gao MZ, Jia ZQ, Xie J (2018) Deformation damage and energy evolution characteristics of coal at different depths. *Rock Mech Rock Eng* 52(5):1491–1503
- Zhao B, Cao J, Sun HT, Wen GC, Dai LC, Wang B (2019) Experimental investigations of stress-gas pressure evolution rules of coal and gas outburst: a case study in Dingji coal mine, China. *Energy Sci Eng* 8(1):61–73
- Zheng YF, Zhai C, Zhang JG, Yu X, Xu JZ, Sun Y, Cong YZ, Tang W (2022) Deformation and fracture behavior of strong–weak coupling structure and its application in coal roadway instability prevention. *Fatigue Fract Eng Mater Struct* 45(1):203–221
- Zhou FB, Xia TQ, Wang XX, Zhang YF, Sun YN, Liu JS (2016) Recent developments in coal mine methane extraction and utilization in China: a review. *J Nat Gas Sci Eng* 31:437–458
- Zhou WL, Zhang PS, Wu RX, Hu XY (2019) Dynamic monitoring the deformation and failure of extra-thick coal seam floor in deep mining. *J Appl Geophys* 163:132–138